

# Strong magnetic response of submicron Silicon particles in the infrared

A. García-Etxarri,<sup>1</sup> R. Gómez-Medina,<sup>2</sup> L. S. Froufe-Pérez,<sup>2</sup>  
C. López,<sup>2</sup> L. Chantada,<sup>3</sup> F. Scheffold,<sup>3</sup> J. Aizpurua,<sup>1</sup>  
M. Nieto-Vesperinas<sup>2</sup> and J. J. Sáenz<sup>1,4</sup>

<sup>1</sup> Donostia International Physics Center (DIPC), Paseo Manuel Lardizabal 4, 20018 Donostia-San Sebastian, Spain

<sup>2</sup> Instituto de Ciencia de Materiales de Madrid, CSIC, Campus de Cantoblanco, 28049 Madrid, Spain

<sup>3</sup> Department of Physics, University of Fribourg, Chemin du Muse 3, 1700 Fribourg, Switzerland

<sup>4</sup> Departamento de Física de la Materia Condensada, Universidad Autónoma de Madrid, 28049 Madrid, Spain  
[juanjo.saenz@uam.es](mailto:juanjo.saenz@uam.es)

**Abstract:** High-permittivity dielectric particles with resonant magnetic properties are being explored as constitutive elements of new metamaterials and devices in the microwave regime. Magnetic properties of low-loss dielectric nanoparticles in the visible or infrared are not expected due to intrinsic low refractive index of optical materials in these regimes. Here we analyze the dipolar electric and magnetic response of loss-less dielectric spheres made of moderate permittivity materials. For low material refractive index ( $\lesssim 3$ ) there are no sharp resonances due to strong overlapping between different multipole contributions. However, we find that Silicon particles with refractive index  $\sim 3.5$  and radius  $\sim 200\text{nm}$  present a dipolar and strong magnetic resonant response in telecom and near-infrared frequencies, (i.e. at wavelengths  $\approx 1.2 - 2\mu\text{m}$ ). Moreover, the light scattered by these Si particles can be perfectly described by dipolar electric and magnetic fields, quadrupolar and higher order contributions being negligible.

© 2022 Optical Society of America

**OCIS codes:** (290.5850) Scattering, particles ; (160.1190) Anisotropic optical materials ; (160.3820) Magneto-optical materials.

---

## References and links

1. H. C. van de Hulst, *Light Scattering by small particles* (Dover, New York, 1981).
2. C. F. Bohren and D. R. Huffman, *Absorption and Scattering of Light by Small Particles* (John Wiley & Sons, New York, 1998).
3. M. I. Mishchenko, L. D. Travis and A. A. Lacis, *Scattering, Absorption, and Emission of Light by Small Particles* (Cambridge Univ. Press, 2002).
4. L. Novotny and B. Hecht, *Principles of Nano-Optics*, (Cambridge University Press, Cambridge, 2006).
5. E. M. Purcell and C. R. Pennypacker, "Scattering and Absorption of Light by Nonspherical Dielectric Grains," *Astrophys. J.* **186**, 705-714 (1973).
6. B. T. Draine, "The discrete dipole approximation and its application to interstellar graphite grains," *Astrophys. J.* **333**, 848-872 (1988).

7. W. L. Barnes, A. Dereux, and T. W. Ebbesen, "Surface plasmon subwavelength optics," *Nature* **424**, 824-830 (2003).
8. N. Engheta and R.W. Ziolkowski, "A Positive Future for Double-Negative Metamaterials," *IEEE Trans. Microw. Theory Tech.* **53**, 1535-1556 (2005).
9. J.B. Pendry, "Beyond metamaterials," *Nature Mater.* **5**, 763 (2006).
10. V. M. Shalaev, "Optical negative-index metamaterials," *Nature Photon.* **1**, 41-48 (2007).
11. P. J. Schuck, D. P. Fromm, A. Sundaramurthy, G. S. Kino, and W. E. Moerner, "Improving the mismatch between light and nanoscale objects with gold bowtie nanoantennas," *Phys. Rev. Lett.* **94**, 017402 (2005).
12. F. Neubrech, A. Pucci, T. W. Cornelius, S. Karim, A. Garca-Etxarri, and J. Aizpurua, "Resonant plasmonic and vibrational coupling in a tailored nanoantenna for infrared detection," *Phys. Rev. Lett.* **101**, 157403 (2008).
13. T. H. Taminiau, F. D. Stefani, F. B. Segerink, and N. F. Van Hulst, "Optical antennas direct single-molecule emission," *Nat. Photonics* **2**, 234237 (2008).
14. A. Alù and N. Engheta, "The quest for magnetic plasmons at optical frequencies," *Opt. Express* **17**, 5723-5730 (2009).
15. A. Alù, and N. Engheta, "Dynamical theory of artificial optical magnetism produced by rings of plasmonic nanoparticles," *Phys. Rev. B* **78**, 085112 (2008).
16. K. C. Huang, M. L. Povinelli, and J. D. Joannopoulos, "Negative effective permeability in polaritonic photonic crystals," *Appl. Phys. Lett.* **85**, 543 (2004).
17. M. S. Wheeler, J. S. Aitchison, J. I. L. Chen, G.A. Ozin, and M. Mojahedi, "Infrared magnetic response in a random silicon carbide micropowder," *Phys. Rev. B* **79**, 073103 (2009).
18. L. Jyhlä, I. Kolmakov, S. Maslovski and S. Tretyakov, "Modeling of isotropic backward-wave materials composed of resonant spheres," *J. Appl. Phys.* **99**, 043102 (2006).
19. L. Peng, L. Ran, H. Chen, H. Zhang, J. A. Kong, and T. M. Grzegorzczak, "Experimental Observation of Left-Handed Behavior in an Array of Standard Dielectric Resonators," *Phys. Rev. Lett.* **98**, 157403 (2007).
20. J. A. Schuller et al., "Dielectric Metamaterials Based on Electric and Magnetic Resonances of Silicon Carbide Particles," *Phys. Rev. Lett.* **99**, 107401 (2007).
21. K. Vynck, D. Felbacq, E. Centeno, A. I. Cabuz, D. Cassagne, and B. Guizal, "All-Dielectric Rod-Type Metamaterials at Optical Frequencies," *Phys. Rev. Lett.* **102**, 133901 (2009).
22. R. K. Mongia, and P. Bhartia, "Dielectric resonator antennas-A review and general design relations for resonant frequency and bandwidth," *Int. J. Microwave Millimeter-Wave Comput.-Aided Eng.* **4**, 230247 (1994).
23. R. C. J. Hsu, A. Ayazi, B. Houshmand, and B. Jalali, "All-dielectric photonic-assisted radio front-end technology," *Nat. Photonics* **1**, 535538 (2007).
24. Jon A. Schuller and Mark L. Brongersma, "General properties of dielectric optical antennas," *Opt. Express* **17**, 24084-24095 (2009).
25. Q. Zhao, J. Zhou, F. Zhang, D. Lippens, "Mie resonance-based dielectric metamaterials," *Materials Today* **12**, 60-69 (2009).
26. E.D.Palik, *Handbook of Optical Constants of Solids* (Academic Press, Orlando, Florida, 1985).
27. S. Albaladejo, R. Gómez-Medina, L. S. Froufe-Pérez, H. Marinchio, R. Carminati, J. F. Torrado, G. Armelles, A. García-Martín and J.J. Sáenz, "Radiative corrections to the polarizability tensor of an electrically small anisotropic dielectric particle," *Opt. Express* **18**, 3556 (2010).
28. P.D. García, R. Sapienza, A. Blanco, and C. López, "Photonic Glass: A Novel Random Material for Light," *Adv. Mater.* **19**, 2597-2602 (2007).
29. M. Reufer, L.F. Rojas-Ochoa, S. Eiden, J.J. Sáenz and F. Scheffold, "Transport of Light in Amorphous Photonic Materials," *Appl. Phys. Lett.* **91**, 171904 (2007).
30. M. Ibisate, D. Golmado and C. López, "Photonic Crystals: Silicon Direct Opals," *Adv. Mater.* **28**, 2899 - 2902 (2009)
31. S. Albaladejo, M.I. Marqués, M. Laroche and J.J. Sáenz "Scattering Forces from the Curl of the Spin Angular Momentum of a Light Field," *Phys. Rev. Lett.* **102**, 113602 (2009).
32. P.C. Chaumet and A. Rahmani, "Electromagnetic force and torque on magnetic and negative-index scatterers," *Opt. Express* **17**, 2224-2234 (2009).
33. M. Nieto-Vesperinas, J.J. Sáenz, R. Gómez-Medina and L. Chantada, "Optical forces on small magnetodielectric magnetic particles," *Opt. Express* **18**, 11428 (2010).

## 1. Introduction

Electromagnetic scattering from nanometer-scale objects has long been a topic of great interest and relevance to fields from astrophysics or meteorology to biophysics and material science [1, 2, 3, 4, 5, 6]. During the last decade nano-optics has developed itself as a very active field within the nanotechnology community. Much of it has to do with plasmon (propagating) based subwavelength optics and applications [7], the synthesis of negative-index optical metamateri-

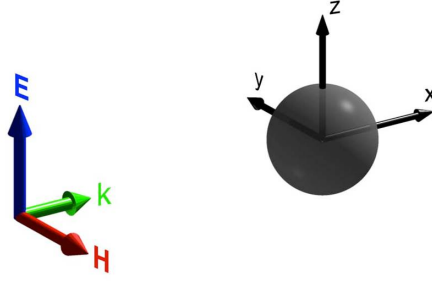


Fig. 1. Incident field vector

als [8, 9, 10] or the design of optical antennas [11, 12, 13].

Magnetic effects, a key ingredient of relevant microwave applications, cannot be easily exploited in the optical range (visible or infrared) due to intrinsic natural limitations of optical materials. The quest for magnetic plasmons and magnetic resonant structures at optical frequencies [14] has been mainly focused on metallic structures with the unavoidable problems of losses and saturation effects inherent to metals in the optical range. Moreover, their size is often required to be comparable to, or a fraction of, the operating wavelength in order to provide a non-negligible response, and their magnetic response is strongly affected and influenced by an intrinsic quadrupolar contribution, which introduces additional radiation losses and impurity of radiation and polarization [15].

As an alternative approach, there is a growing interest in the theoretical and experimental study of high-permittivity dielectric objects as constitutive elements of new metamaterials [16, 17, 18, 19, 20, 21] and antennas based on dielectric resonators [22, 23, 24]. Interesting magnetodielectric properties are usually associated to low loss and large dielectric constants which, being accessible at microwave and terahertz frequencies, are still a challenging issue in the infrared (IR) and visible frequency ranges [25]. However, it has recently been shown [21] that silicon rod arrays could exhibit a true metamaterial left handed dispersion branch in the visible to mid-IR despite the moderate value of the refractive index ( $m \sim 3.5$ ).

Motivated by these results, we have analyzed in detail the magnetodielectric properties of loss-less dielectric spheres made of moderate permittivity materials in the infrared regime. Although the analysis of scattering resonances of homogeneous spheres have been analyzed in the past [1, 2, 3], we concentrate here on the relevance of the first magnetic dipolar resonance in non-absorbing dielectric nano-spheres (e.g. silicon spheres in the mid-IR). As we will see, submicron Silicon spheres (with radius  $a \approx 200\text{nm}$ ) can present a strong magnetic resonance response at telecom and infrared frequencies, (namely, wavelengths  $\lambda \approx 2na \approx 1.5\mu\text{m}$ ). Moreover, based on standard Mie theory [1], we have found that *the scattering of these Si nanoparticles can be perfectly described by dipolar electric and magnetic fields; quadrupolar and higher order contributions being negligible*. Interestingly, the magnetic resonance line remains well defined and resolved even for lower index materials, as Rutile-like  $\text{TiO}_2$  with an average index  $m \approx 2.8$  in the near-IR, even though in this latter case the electric dipole resonance line strongly overlaps with the magnetic dipole one, as well as with those of higher order multipoles.

## 2. Extinction resonances of a dielectric sphere. The Mie theory revisited

Consider a non-absorbing dielectric sphere of radius  $a$ , index of refraction  $m_p$  and dielectric permittivity  $\epsilon_p = m_p^2$  in an otherwise uniform medium with real relative permittivity  $\epsilon_h$  and re-

fractive index  $m_h = \sqrt{\epsilon_h}$ . The magnetic permittivity of the sphere and the surrounding medium is assumed to be 1. Under plane wave illumination, and assuming linearly polarized light, the incident wave is described by

$$\mathbf{E} = E_0 \mathbf{u}_Z e^{ikX} e^{-i\omega t} \quad , \quad \mathbf{B} = B_0 \mathbf{u}_Y e^{ikX} e^{-i\omega t} \quad (1)$$

where  $k = m_h \omega / c = m_h 2\pi / \lambda$ ,  $\lambda$  being the wavelength in vacuum and  $B_0 = \mu_0 H_0 = -(m_h / c) E_0$  (see Fig. 1). The field scattered by the sphere can be decomposed into a multipole series, (the so-called Mie's expansion), characterized by the electric and magnetic Mie coefficients  $\{a_n\}$  and  $\{b_n\}$ , respectively; ( $a_1$  and  $b_1$  being proportional to the electric and magnetic dipoles,  $a_2$  and  $b_2$  to the quadrupoles, and so on). We shall find useful to write the Mie coefficients in terms of the scattering phase-shifts  $\alpha_n$  and  $\beta_n$  [1]

$$a_n = \frac{1}{2} (1 - e^{-2i\alpha_n}) = i \sin \alpha_n e^{-i\alpha_n} \quad (2)$$

$$b_n = \frac{1}{2} (1 - e^{-2i\beta_n}) = i \sin \beta_n e^{-i\beta_n} \quad (3)$$

where

$$\tan \alpha_n = \frac{m^2 j_n(y) [x j_n(x)]' - j_n(x) [y j_n(y)]'}{m^2 j_n(y) [x y_n(x)]' - y_n(x) [y j_n(y)]'} \quad (4)$$

$$\tan \beta_n = \frac{j_n(y) [x j_n(x)]' - j_n(x) [y j_n(y)]'}{j_n(y) [x y_n(x)]' - y_n(x) [y j_n(y)]'} \quad (5)$$

$m = m_p / m_h$  being the relative refractive index,  $x = ka$  the size parameter and  $y = mx$ .  $j_n(x)$  and  $y_n(x)$  stands for the spherical Bessel and Neumann functions, respectively, and the primes indicate differentiation with respect to the argument. In absence of absorption, i.e. for real  $m$ , the phase angles  $\alpha_n$  and  $\beta_n$  are real, then the extinction and scattering cross sections,  $\sigma_{\text{ext}}$  and  $\sigma_S$ , respectively, have the common value [1]

$$\sigma_S = \sigma_{\text{ext}} = \frac{2\pi}{k^2} \sum_{n=1}^{\infty} (2n+1) \{ \sin^2 \alpha_n + \sin^2 \beta_n \} = \sum_{n=1}^{\infty} \{ \sigma_{E,n} + \sigma_{M,n} \} \quad (6)$$

In the small particle limit ( $x \ll 1$ ) and large particle permittivities ( $m \gg 1$ ) the extinction cross section presents characteristic sharp resonance peaks. The values of  $y = mx$  at which the angles  $\alpha_n$  or  $\beta_n$  are  $\pi/2, 3\pi/2, \dots$ , etc, define the resonance points. At each resonance, the extinction cross section is of the order of  $\lambda^2$  and it is independent of either the particle size or the refractive index [1]

$$\sigma_S^{\text{res}} = \sigma_{\text{ext}}^{\text{res}} |_{\{x \ll 1; m \gg 1\}} \approx \frac{2\pi}{k^2} (2n+1) \quad (7)$$

Asymptotically, the first resonance peak occurs at  $y = \pi$  (i.e.  $\lambda = m2a$ ) corresponding to the magnetic dipole term of coefficient  $b_1$ .

Interesting consequences and applications of well defined Mie resonance lines, associated to low loss and large dielectric constants, are accessible for different materials at microwave and terahertz frequencies. However, as  $m$  decreases there is an increasing overlap between the wavelength dependent cross-section peaks, and the sphere resonant response smears out. Since usually non-absorbing materials present low refractive index in the infrared (IR) and visible frequency ranges, Mie resonances of small particles in these regimes have not been considered in detail. However, the above analysis on the cross-section, carried out for Si nanoparticles

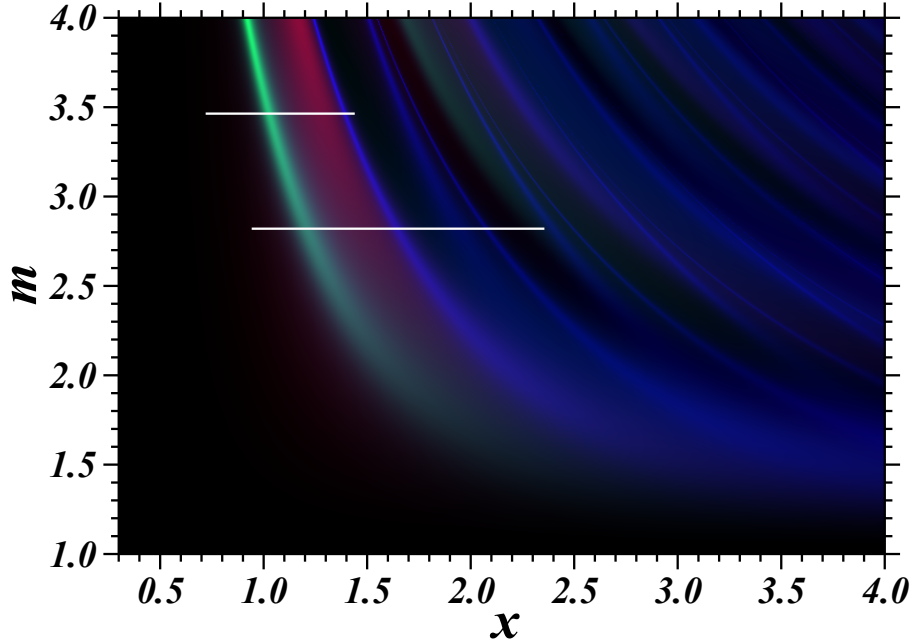


Fig. 2. Scattering cross section map of a non-absorbing Mie sphere as a function of the refractive index  $m$  and the size parameter  $x = 2\pi a/\lambda$ . Green areas correspond to parameter ranges where the magnetic dipole contribution dominates the total scattering cross section, while red areas represent regions where the electric dipole contribution is dominating. The remaining blue-saturated areas are dominated by higher order multipoles. Brightness in the color-map is proportional to the total cross section. White horizontal lines represent the  $x$ -range covered by figures 3 ( $m = 3.5$ ) and 5 ( $m = 2.8$ )

in the IR, indicate that the aforementioned asymptotic behavior can be extended to a relative refractive index as low as  $m \approx 3$ .

In Fig. 2 we show the scattering cross section map of a non-absorbing Mie sphere as a function of the refractive index  $m$  and the size parameter  $x = 2\pi a/\lambda$ . Brightness in the color-map is proportional to  $\sigma_{\text{ext}}$  while color code represents the contribution of electric and magnetic dipoles to the total cross section. The RGB (Red, Green, Blue) code is formed by taking  $RGB = \sigma_{E,1}R + \sigma_{M,1}G + \sigma_{\text{res}}B$  with  $\sigma_{\text{res}} \equiv \sqrt{\sigma_{\text{ext}}^2 - \sigma_{E,1}^2 - \sigma_{M,1}^2}$ . The whole map is normalized to avoid over-saturation. Hence, green areas correspond to parameter ranges where the magnetic dipole contribution dominates the total scattering cross section, while red areas represent regions where the electric dipole contribution is dominating. The remaining blue-saturated areas are dominated by higher order multipoles.

In the micrometer wavelength regime, within the transparent region of silicon ( $\lambda \gtrsim 1100$  nm), the index of refraction can well be approximated by a real constant  $m_p \approx \sqrt{12} \sim 3.5$  (see for example [26]). The scattering (or extinction) cross section of a Si sphere of radius  $a = 230\text{nm}$  in vacuum ( $m_h = 1$ ) is plotted in Fig. 3. Although there is a partial overlap between the first dipolar peaks, the magnetic line of the first resonant peak (at  $\lambda \approx 2ma$ ) is still very well resolved. Interestingly, for wavelengths larger than  $\lambda \approx 1200\text{nm}$ , the cross section is completely determined by the first  $b_1$  and  $a_1$  coefficients. In other words, in this regime Si particles can be treated as non-Rayleigh dipolar particles.

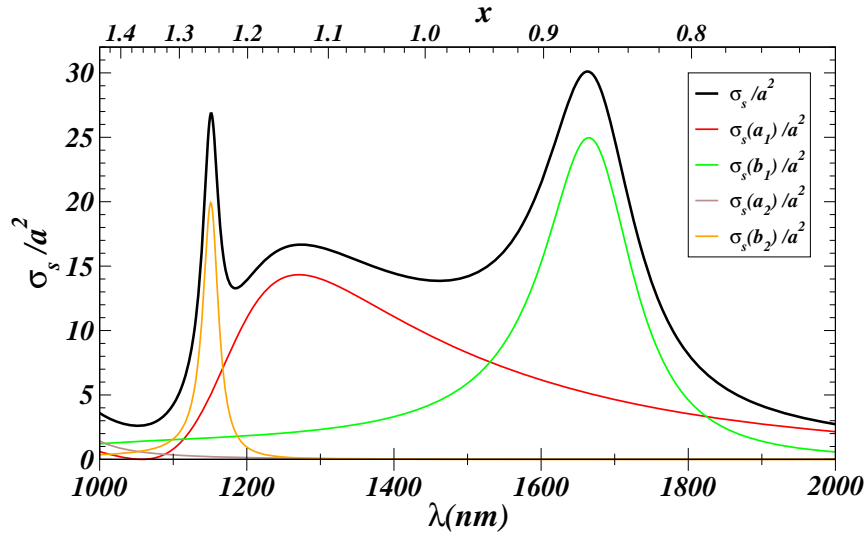


Fig. 3. Scattering cross-section  $\sigma_s$  versus the wavelength  $\lambda$  for a 230nm Si sphere (the refraction index  $m = 3.5$  is constant and real in this wavelength range). The contribution of each term in the Mie expansion is also shown. The green line corresponds to the magnetic dipole contribution.

### 3. Magnetic and electric resonances of dipolar particles

Let us consider further in some detail the scattering properties of small dielectric particles ( $x \ll 1$ ). In the  $x \ll 1$  limit, the sphere is sufficiently small so that only the dipole scattered fields are excited. The induced dipole moments, proportional to the external (polarizing) fields,  $\mathbf{E}$  and  $\mathbf{B}$ , are usually written in terms of the particle electric and magnetic polarizabilities  $\alpha_E$  and  $\alpha_M$ , respectively :

$$\mathbf{p} = \epsilon_0 \epsilon_h \alpha_E \mathbf{E} \quad , \quad \mathbf{m} = \epsilon_0 \epsilon_h \alpha_M \mathbf{B}; \quad (8)$$

where

$$\alpha_E = i \left( \frac{k^3}{6\pi} \right)^{-1} a_1 \quad , \quad \alpha_M = i \left( \frac{k^3}{6\pi} \right)^{-1} b_1. \quad (9)$$

By using the definition of the phase angles  $\alpha_1$  and  $\beta_1$ , [cf. Eqs. (2) - (5)], we can rewrite the polarizabilities as

$$\alpha_E = \frac{\alpha_E^{(0)}}{1 - i \frac{k^3}{6\pi} \alpha_E^{(0)}} \quad , \quad \alpha_M = \frac{\alpha_M^{(0)}}{1 - i \frac{k^3}{6\pi} \alpha_M^{(0)}}, \quad (10)$$

where

$$\alpha_E^{(0)} = -\frac{6\pi}{k^3} \tan \alpha_1 \quad , \quad \alpha_M^{(0)} = -\frac{6\pi}{k^3} \tan \beta_1 \quad (11)$$

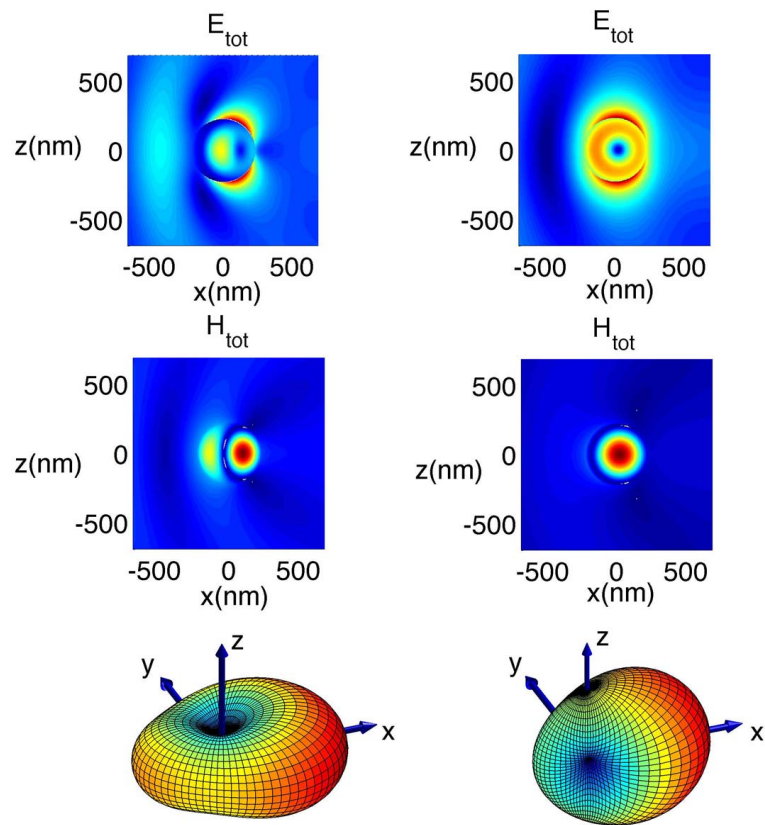


Fig. 4. Maps for the square modulus of the total electric and magnetic vectors, emitted by the Si nanoparticle of radius  $a = 230\text{nm}$  under plane wave illumination, (cf. Fig. 1). The left and right panels correspond to the wavelengths  $1250\text{nm}$  and  $1680\text{nm}$  of the electric and magnetic resonance peaks of Fig. 3, respectively. The corresponding far field radiation patterns are shown in the bottom.

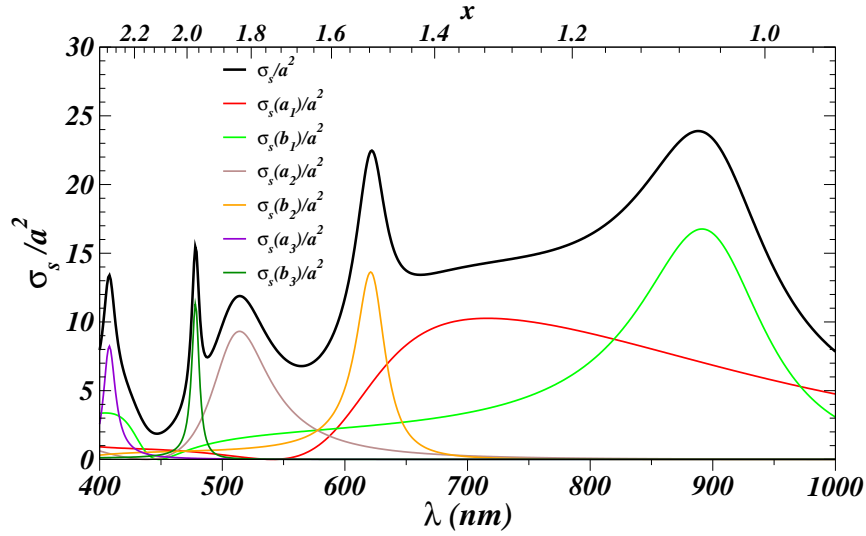


Fig. 5. Scattering cross-section  $\sigma_S$  versus the wavelength  $\lambda$  for a sphere of radius  $a = 150\text{nm}$  (its relative refractive index is  $m = \sqrt{8} = 2.82$ , constant and real in this wavelength range). The contribution of each coefficient in the Mie expansion is also shown. The green line corresponds to the magnetic dipole contribution.

are the quasi-static polarizabilities. In terms of these magnitudes, the extinction and scattering cross sections then read

$$\sigma_{\text{ext}} = k \text{Im} \{ \alpha_E + \alpha_M \} \quad (12)$$

$$\sigma_S = \frac{k^4}{6\pi} \left\{ |\alpha_E|^2 + |\alpha_M|^2 \right\} \quad (13)$$

Of course, in absence of absorption,  $\alpha_E^{(0)}$  and  $\alpha_M^{(0)}$  are real quantities and we recover the well known *optical theorem* result  $\sigma_{\text{ext}} = \sigma_S$ .

In particular, in the Rayleigh limit, when  $y \equiv 2\pi ma/\lambda \ll 1$ ,  $\alpha_E^{(0)}$  and  $\alpha_M^{(0)}$  approach the electrostatic form,

$$\alpha_E^{(0)} \Big|_{y \ll 1} \approx 4\pi a^3 \frac{m^2 - 1}{m^2 + 2} \quad , \quad \alpha_M^{(0)} \Big|_{y \ll 1} \approx 4\pi a^3 (m^2 - 1) \frac{k^2 a^2}{30} \quad (14)$$

From Eq. (14), together with Eq. (10), we recover the well known expression for the polarizability of a Rayleigh particle including radiative corrections [6, 27]. Notice that in this limit the magnetic polarizability is negligible. Very small particles always behave as point electric dipoles.

However, as  $y$  increases, (i.e. as  $\lambda$  decreases), there is a crossover from electric to magnetic behavior as shown by Fig. 3 for a Si particle. The  $y$  values at which the quasi-static polarizability  $\alpha_E^{(0)}$  ( $\alpha_M^{(0)}$ ) diverges define the electric (magnetic) dipolar resonances. Near the first

$b_1$ -resonance, the particle essentially behaves like a magnetic dipole (cf. Fig. 2). If  $\lambda$  decreases further,  $a_1$  peak dominates and the sphere becomes again an electric dipole. Notice however that, due to the overlap between the electric and magnetic responses, the radiation field near the resonances does not correspond to a fully pure electric or a fully pure magnetic dipolar excitation. Yet, as seen in Fig.2 for the aforementioned Si sphere, the magnetic dipole contribution is, at its peak, about five times larger than the electric dipole one.

As a further example, we have plotted in Fig. 4 both the near field intensity maps and far field radiation patterns at the resonant peaks of  $a_1$  and  $b_1$ , (cf. Fig. 3), numerically calculated from the full Mie solution (and not only from the dipolar approximation). The slightly distorted patterns with respect to the single dipole case are completely explained in terms of the sum of these two mutually coherent electric and magnetic dipoles.

Silicon nanoparticles with radius of the order of 200-250nm are then fully characterized by electric and magnetic polarizabilities as given by Eqs. 10 in the mid and near-IR region. By tuning the appropriate resonance wavelength, Si particles exhibit a strong magnetic response, (only slightly perturbed by their electric dipole counterpart).

It should be remarked that if the relative refractive index is smaller, the overlap between the Mie resonance lines increases and then, a particular one single Mie term magnetic response is not well defined. As an example, in Fig. 5 we represent the scattering cross section of a 150nm radius particle with  $m = \sqrt{8} \approx 2.8$  (which would be of the order of the averaged refractive index of TiO<sub>2</sub> (rutile) in the near IR [26]). As seen in this figure, although beyond 700nm the scattering is still described by the sum of the electric and magnetic dipoles, the peak corresponding to the electric dipole,  $a_1$ , now disappears, and the overlapping between lines that produces this, manifests a significant contribution of this electric dipole at the magnetic resonance wavelength.

#### 4. Conclusion

We have analyzed the dipolar electric and magnetic response of lossless dielectric spheres made of both low and moderate permittivity materials. Based on the Mie expansion, we have derived general expressions for the electric and magnetic polarizabilities of dielectric spheres. We found that submicron Silicon particles present a strong magnetic resonant response in the mid-near infrared. Interestingly, *the light scattered by these Si nanoparticles of appropriate size is perfectly described by dipolar electric and magnetic fields, being quadrupolar and higher order contributions negligible*. These results can play an important role, not only in the field of metamaterials or optical antennas, but also in tailoring the light transport through complex dielectric media like photonic glasses [28, 29] with intriguing magnetic properties. Fabrication of new materials made of highly monodisperse subwavelength silicon spheres [30] may then lead to a new generation of magnetodielectric optical materials. At the magnetic or electric resonance wavelengths the extinction cross section is of the order of  $\lambda^2$  reaching its maximum theoretical limit (independent of the particle size or refractive index) [1] ( see also [24] ). The large dipolar cross-section of magnetodielectric spheres near a magnetic resonance would also imply strong radiation pressure magnetic forces [31, 32, 33] leading to new concepts related to the optical forces on magnetic particles .

#### Acknowledgement

We appreciate interesting discussions with S. Albaladejo, F. González, L. Inclán, F. Moreno, J.M. Saiz, I. Suárez and K. Vynck. This work has been supported by the EU NMP3-SL-2008-214107-Nanomagma and NoE Nanophotonics4Energy 248855, the Spanish MICINN Consolider *NanoLight* (CSD2007-00046), MAT2009-07841 GLUSFA and FIS2009-13430-C02-02 and by the Comunidad de Madrid Microseres-CM (S2009/TIC-1476) and PHAMA-CM (S2009/MAT-1756). F.S. and L.C. acknowledge financial support from the Swiss National Sci-

ence Foundation, Projects No. 126772 and 117762. Work by R.G.-M. and L.S.F.-P. was supported by the MICINN "Juan de la Cierva" Fellowship.